IEEE Access
Multidisciplinary | Rapid Review | Open Access Journal

Received July 6, 2019, accepted July 23, 2019, date of publication July 29, 2019, date of current version September 4, 2019.

Digital Object Identifier 10.1109/ACCESS.2019.2931742

A Hybrid Many-Objective Evolutionary Algorithm With Region Preference for Decision Makers

MINGHUI XIONG, WEI XIONG, AND CHENGXIANG LIU

Science and Technology on Complex Electronic System Simulation Laboratory, Space Engineering University, Beijing 101416, China

Corresponding author: Minghui Xiong (xtkxxmh@163.com)

This work was supported by the Key Laboratory Foundation under Grant 614201003010517.

ABSTRACT In many-objective optimization, maintaining a good balance between convergence and diversity have turned out to be a considerable challenge for classical evolutionary algorithms. The large scale solution set required to describe the entire Pareto optimal front hinder the decision makers from finding the most satisfactory solution, whereas he/she is only interested in a limited part of the objective space. The dilemma can be handled by incorporating the preference information in the search process. In this paper, an evolutionary algorithm based on region preference is proposed for many-objective optimization. The preference model is constructed in combination of the target region and reference points. To focus the search on the preference region while maintaining well convergence and diversity within the region, a tri-level ranking criterion is introduced into the proposed algorithm, and different rank works at different phase of the search process. A fuzzy theory-based interactive approach is proposed to guide more individuals to further search into the objective space with higher preference degree and help the decision maker choose the most interested solution. The proposed algorithm has been extensively compared with other state-of-the-art preference-based algorithms on DTLZ1∼ DTLZ4 test problems having 3-10 objectives. The experimental results indicate that the proposed algorithm can achieve competitive and better performance. Moreover, we extend the algorithm to handle multiple target regions.

INDEX TERMS Many-objective optimization, evolutionary algorithm, preference articulation, interactive approach.

I. INTRODUCTION

Many problems in the fields of natural sciences, social sciences, and engineering practice include multiple objectives to be optimized, such as flow shop scheduling problem [1] and portfolio optimization problem [2], etc. Generally, the multi-objective optimization problem with more than three objective dimensions is defined as many-objective optimization problem (MaOPs) [3]. The aim of solving MaOPs is deemed as helping the decision makers (DM) in finding the most preferred solution. The existing multi-objective evolutionary algorithm (MOEAs) perform steadily on problems with two or three objectives. However, the Pareto dominance-based algorithms have suffered great difficulties with the increasing number of objectives. The primary reason attributes to the dominance resistance [4], where most candidate solutions become mutually non-dominated, hence lead to the severe loss of the selection pressure. Moreover, it is often difficult for decision makers to visually understand the trade-off between four-dimensional and above objectives, which means it difficult to select the optimal solution from the large scale solution set [5].

Most MOEAs attempt to discover the entire Pareto optimal front at a large computational cost. Whereas in context of real-world optimization problems, the decision makers are often interested in a limited part of the objective space. Seen from the perspective of DM, these algorithms waste too much computational resource acquiring unnecessary solutions. Hence some researchers incorporate the DM's preference information to guide the search into the most interested region instead of the whole Pareto front. In this way, the selection pressure is enhanced while alleviating the selection burden of the

The associate editor coordinating the review of this article and approving it for publication was Dusmanta Kumar Kumar Mohanta.

DM. Most existing many-objective optimization algorithms utilize the preference information before (a-priori) or after (a-posteriori) the search process, but seldom of them are designed to be interactive. Usually, the DM lacks a priori information of the trade-off between objectives, and the true Pareto front located within the preset target region may be empty. The interactive approach makes it possible to change the preference information during the search process for a more reasonable solution set. So we should introduce an interactive approach, which is one of starting points of our proposed algorithm.

The preference information can be articulated through desirability function[6], [7], preference region [8], weight adaption [9], reference point [10], outranking relation [11], performance indicators (R2-indicator [12], averaged Hausdorff distance [13]) and so on. Among these preference-based multi-objective evolutionary algorithms (PMOEAs), the reference points-based MOEAs perform the predefined targeted search by means of predefined reference points, which can effectively alleviate several difficulties in handling many objectives; the preference region-based method define the region in shape of a rectangle or a circle and the preference range on each objective is controllable, making it a more intuitive and flexible way for DM to express preference. However, most of the existing interactive approaches produce a single reference point, which is in dilemma to real-word application.

In this paper, we propose a hybrid interactive many-objective optimization evolutionary algorithm with region preference for decision makers. The preference model combines the target region and reference point together, based on which the DM can intuitively express his/her preference and guide the search process to the most interested region. The main contributions of this paper can be summarized as follows.

- We construct a preference model which reflects the preference information of DM, then a corresponding tri-level ranking criterion is designed to focus the search process on the preference region while balancing convergence and diversity of the solution set.
- Fuzzy theory is utilized in interactive approach to further guide the solutions reach to the objective with higher preference degree, assist the DM in understanding the distribution pattern of preferred solutions and finding the most preferred solutions.
- Performance comparison is conducted against two state-of-the-art algorithms on DTLZ test suit with multiple target regions to demonstrate the efficacy and usefulness of the proposal.

The remainder of this paper is organized as follows. In Section II, we introduce the background knowledge, a summary of state-of-the-art works and a visual clustering approach to visually judge the performance of the preference-based algorithms. The proposed algorithm is described in detail in Section III. Section IV shows the experimental evaluation of the proposed method and comparisons with two recently proposed preference region-based algorithms. Finally, the conclusion is drawn in Section V.

II. PRELIMINARIES

In this section, some basic definitions in multi-objective optimization are first given. Then, we summarize the recently improvement in preference-based algorithms, especially reference point-based and preference region-based approaches. Finally, a visual clustering method is introduced to visually inspect the effectiveness of PMOEAs in Section IV.

A. BASIC DEFINATIONS

In this study, the following multi-objective optimization problem can be mathematically defined as

$$\begin{cases} \min\ F(x) = (f_1(x), \quad f_2(x), \ldots, f_N(x)) \\ subject\ to\ g_i(x) \le 0 \quad i = 1, 2, \ldots, p \end{cases} \tag{1}$$

where $x \in \Omega$ is called the decision vector, and Ω is a continuous search space. $N \ge 2$ is the number of the objective functions, and p is the number of constrains. $F : x \to R^N$ is the map of decision variable space to N real valued objective space.

Definition 1. (Pareto Dominance): Given two decision vectors $x, y \in \Omega$, x is said to Pareto dominate y, denoted by $x \prec y$, iff $f_i(x) \le f_i(y)$, for every $i \in \{1, 2, \ldots, N\}$, and $f_j(x) \le f_j(y)$, for at least one index $j \in \{1, 2, \ldots, N\}$.

Definition 2. (Pareto Optimality): A solution x^* is Pareto optimal iff there is no $x \in \Omega$ such that $x \prec x^*$.

Definition 3 (Pareto Set): For a given MOP $F(x)$, the Pareto set (PS) is defined as

$$\mathrm{PS} = \{x \in \Omega \,|\, x \text{ is Pareto optimal}\} \tag{2}$$

Definition 4. (Pareto Pront): The Pareto front (PF) is defined as

$$\mathrm{PF} = \left\{ f(x) \in \mathrm{R}^N \,|\, x \in \mathrm{PS} \right\} \tag{3}$$

B. REFERENCE POINT-BASED APPROACHES

The reference point-based approach employs a set of predefined reference points to perform the predefined targeted research. The distribution of the reference point represents the aspiration level of the DM on each objective.

MOGA [14] developed by Fonseca and Fleming is considered as the earliest such approach. A goal vector is utilized to specify the aspiration levels and attach priority to solutions satisfying the goals. MOGA was further extended by [15], [16] in introducing a preferability operator and a goal-sequence domination scheme. The main weakness of this method is that it requires prior information of objective value ranges so as to initialize the goal vector. Another widely used approach, proposed by Molina et al. [17] is a dominance relation named g-dominance. In g-dominance, solutions satisfying all aspirations or none of the aspirations are preferred over solutions satisfying some aspirations. But g-dominance faces difficulties in handling multiple ROIs for a solution

can g-dominance one goal vector, and simultaneously, be g-dominated by another goal vector [18].

Goulart and Campelo [19] employ a single reference point to express the preferences of a decision maker, and adaptively biases the search procedure toward the region of the Pareto-optimal front that best matches its expectations. But it is still insufficient to express preference degree or precisely control preference region using only a single reference point. In [20], a positive point is utilized to divide the search space and converge the population to the preference area, while a negative point works discourage the solutions close to the negative preference. NSGA-III [21] generates a set of well-spread reference points towards the entire PF. But under the condition that replacing the uniform points with DM-defined reference points, it can also focus on the preferred part of PF. Motivated by the clustering operation in NSGA-III, Cai *et al.* [22] cluster each solution based on the minimum vertical distance to its corresponding reference line, then the ranking operator works to accelerate the convergence pace. Zhao and Liu [23] project these uniformly distributed point into the preference region using the information of reference point and the preference angle, in which way the guidance of search process is more specifically described.

Reference points can also hybrid with the indicator-based algorithms, where the predefined points are applied to an achievement scalarizing function incorporated into the indicator function. In R2-indicator, the preference is articulated by the distribution of reference points. Gómez and Coello cut-off the objective space through adaptively updating the reference points taking the statistical information of previous generations into account [24]. The Aspiration Set EMOA [25] considers a set of reference points to guide the search, with averaged Hausdorff distance as the quality indicator.

C. PREFERENCE REGION-BASED APPROACHES

In preference region-based approaches, Solutions located in the preferred region and uninterested region are then assigned different territories such that more solutions are obtained within the region of interest (ROI). The ROI can be defined either in an explicit form (such as target region [26], desirability function [27], etc.), or an indirect form (such as weight vector [28], reference vector [29], etc.).

Desirability function maps the objectives to the interval [0, 1] according to their desired value. The search process can be guided to different part of the PF through changing the objective values corresponding to desired value 0 and 1. Trautmann and Mehnen [27] incorporate Harrington's one side desirability function in NSGA-II for focusing on interested PF in noisy environment. In [30], DF is integrated into the hypervolume-based selection. For the purpose of extending DF to many-objective optimization, they take desirability index, which is of low computational complexity, as the second-level selection criterion in the non-dominated sorting [31].

Jiao and Zhang [8] propose the concept of region-dominance. Different from the nonlinearly transformation in DF, the desired value of solutions within the region is assigned 1, while the outside ones is assigned 0. It enables the DM to obtain an effcient set of solutions in his/her preferred region without using any scalarizing function. Wang and Li [32] adapt this idea and present the target region in the objective space in the shape of a rectangle or a circle, and proposed a target region-based algorithm family (T-SMS-EMOA, T-R2-EMOA and T-NSGA-II). Numerical comparisons show the capability of the algorithms in finding solutions in a more fine-grained resolution within a predefined target region. In the application of many-objective optimization for agile satellite mission planning, Li *et al.* [33] extend the algorithm family with T-MOEA/D and T-NSGA-III. Compared with the original algorithms, lower bound of the target region in T-MOEA/D and T-NSGA-III is used as the ideal point. It accelerates the evolution process to the target region.

Hybrid with reference vector, preference region construction in RVEA [34] is defined by a central vector and a radius. The adaptively adjusted reference vectors within the preference convex cone lead to the evenly distributed Pareto solution sets. In [35], Gong *et al.* dynamically changing the density of the weight vectors to specify the preference by a hypersphere.

In [36] and [37], reference points are employed as the lower bound of the preference regions. To avoid obtaining only one Pareto optimal solution, an additional threshold is used to control the range of the ROIs.

Among the above preference-based algorithms, we select T-MOEA/D and T-NSGA-III [33] for comparison. They share the preference region definition form with our proposed approach and are designed for many-objective optimization. More details of T-MOEA/D and T-NSGA-III will be described in Section IV.

D. NON-DOMINATED SOLUTIONS VISUALIZATION

Most of the existing studies visually observe the high dimensional non-dominated solution sets using the Parallel Coordinate Plots [38] (PCPs). Each of axes in the parallel coordinate system corresponds to one objective space, and each solution in the M-dimensional objective space is represented by a corresponding M-1 segment polyline. However, the over-crowded polylines intersect and overlap to each other in the plot, which makes it difficult for decision makers to understand the distribution pattern of non-dominated solutions. In this section, we introduce the electromagnetic field physical model into visual clustering, aiming to visually judge the performance of the preference-based algorithms.

Inferred from Ampere's circuital law and Fleming's right hand rule [39], for the current-carrying wires placed in the same plane, the same current direction wires tend to attract each other, while the opposite current directions ones repel each other. Motivated by this phenomenon, the physical model is introduced into the visual clustering process: solutions in the same cluster have the same direction thus

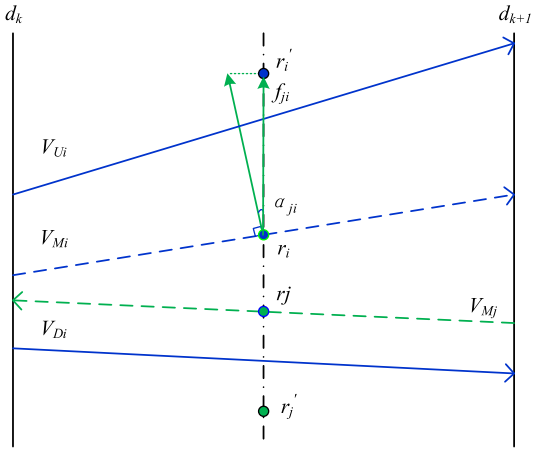

FIGURE 1. Schematic diagram of electromagnetic field clustering method. The solid lines are the bounds of cluster, the dotted line is the center line of cluster.

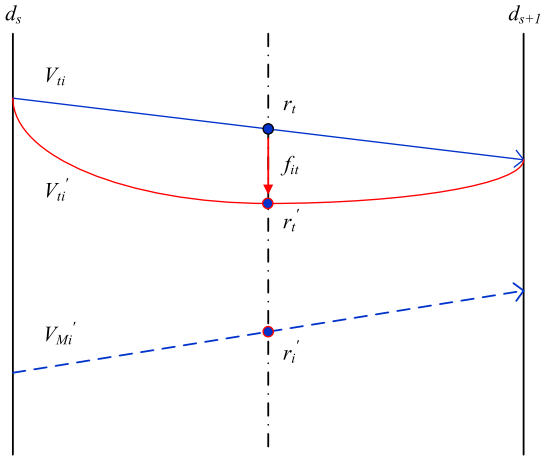

FIGURE 2. Calculation of solution center point coordinate.

attract each other; while the solutions in different clutter have opposite directions and are mutually exclusive. The clustering method based on the electromagnetic field model is shown in Fig. 1.

Between the *k-th* and *k+1-th* dimensional axes, V_{Ui} and V_{Di} are the upper and lower bounds of cluster i; V_{Mi} is the corresponding cluster centerline, and the center point is r_i. V_{Mj} is the centerline of cluster j, and the center point is r_j. To simplify the problem, we only analyze the force and movement of the center point in the y-axis direction. The specific steps of the clustering method are as follows:

1) Calculation of cluster center point coordinate

The initial position of the cluster center point is determined by the mean values of upper and lower bounds of each cluster as $r_i\,(x_i, y_i)$ and $r_j\left(x_j, y_j\right)$. To reduce the staggering and overlapping of inter-cluster lines, the coordinate of center point is adjusted by the repulsive force from other clusters. Referring to the Lorentz force function, we define the cluster repulsive force subjected to other N-1 clusters in (4),

$$f_i = F_r \cdot \sum_{j=1}^{N-1} \frac{n_i \cdot n_j}{\left(n_i + n_j\right)^2} \cdot \cos\alpha_{ji} \cdot H_i \tag{4}$$

$F_r \in [0, 1]$ is the repulsive intensity coefficient, which is used to control the repulsive strength between the cluster center points; n_j represents the number of solutions contained in cluster j; H_i is the length of cluster center line V_{Mi}; α denotes the angle between f_{ji} and the positive direction of y-axis, whose cosine value can reveal the force direction from cluster j to cluster i. Positive fi indicates that cluster i is subjected to upward force, while negative indicates being subjected to downward force; and the larger absolute value of f_i means the greater displacement of r_i, Let the coordinates of center point r_i, after the repulsion be $r_i'\left(x_i', y_i'\right)$.

2) Calculation of solution center point coordinate

The solutions within the same cluster show gravitation to each other, that is, the inner cluster solution center gathers toward cluster center point coordinate. Fig. 2 shows the calculation of solution center point coordinate: V_{ti} is one solution of cluster i, whose corresponding original center point is $r_t\,(x_t, y_t)$.

Subjected to the gravitational force of r_i', assuming r_t moves to $r_t'\left(x_t', y_t'\right)$, then y_t' can be obtained by (5),

$$y_t' = F_g \cdot y_i + \left(1 - F_g\right) \cdot y_t \tag{5}$$

$F_g \in [0, 1]$ is the gravitational intensity coefficient. The larger F_g means the higher aggregation degree. Therefore, the decision maker can adjust the visualization effect by changing F_g.

3) Visualization mapping based on clustering

The input solution set D includes N solutions, and each solution corresponds to an M-1 segment polyline. Therefore, the solution set D corresponds to $N \cdot (M-1)$ solution center point. Repeat steps 1, 2 until all the solution center points between the adjacent axes are obtained. The center point and the end points of the polyline served as the extreme points, we apply cubic spline interpolation to obtain the smooth curve after the clustering process (the red curve in Fig. 2). Thus, the high-dimensional solution is mapped into the two-dimensional parallel coordinate system.

Fig. 3 shows an illustration of visual clustering the true Pareto frontier of the DTLZ3 test problem [40] based on the electromagnetic field clustering method. According to the variation of DM's preference on different parts of the objective space, the entire PF is classified into five categories, and five smooth curves from purple to cyan denote to the preference degree from high to low. When the evolutionary algorithm obtains a non-dominated solution closest to the preferred region, the individual will be represented by the corresponding curve. Therefore, this method can be used to reveal whether the algorithm effectively guides the search process of the solution into the preference region, as well as the distribution pattern of the solutions in different preference regions.

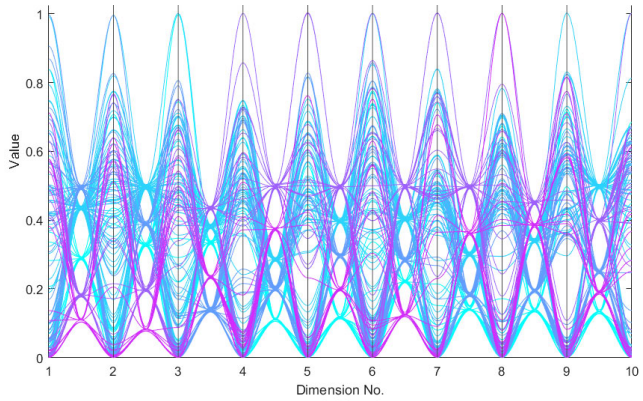

FIGURE 3. Illustration of electromagnetic field visual clustering: 10-objective DTLZ3 problem.

III. PROPOSED ALGORITHM: HMOEA-T

A. OVERVIEW

The framework of the proposed HMOEA-T is described in Algorithm 1. The aim of HMOEA-T is to guide the search to the target region and obtain a well-converged and well-distributed PS within it.

First, the target region is explicitly specified by the lower and upper bounds on each objective. In step 2-3, the preference model is constructed. A set of N uniformly distributed reference points are generated, which can be denoted as $\Lambda = \{\lambda_1, \lambda_2, \ldots, \lambda_N\}$. Then, the original reference points are regulated towards the target region for achieving only the preferred section of the PF. Next, the initial population P_0 with N members is randomly produced. The main loop steps are iterated until the termination criterion is satisfied. In step 8, the offspring population Q_t is produced by using the recombination operator. Then P_t is updated by combining Q_t with the current population. To accelerate the search pace towards the target region while balancing the diversity and convergence, we propose a tri-level ranking criterion. The Pareto non-dominated relationship is utilized as the first ranking criterion, and the population $S_t = \cup_{i=1}^{\tau} F_i$, where F_i is the i_{th} Pareto non-dominated front of P_t and τ satisfies $\sum_{i=1}^{\tau-1} |f_i| < N$ and $\sum_{i=1}^{\tau} |f_i| \geq N$. Number of the non-dominated solutions is directly proportional to the number of objective, when the objective number comes to 20, almost all solutions are mutually non-dominated [5]. So for problems with high number of objectives, S_t is almost always equal to F_1. At early phase of the search, no solutions reach to the target region. In this case, 1st and 3rd criterion work effectively guiding solutions to the target region. In step 11, all the solutions are clustered based on the minimum vertical distance to the reference vector. To attach priority to the solutions close to the region center, we rank the reference points R_{cos} based on the cosine similarity to the region center. Then each solution in S_t is assigned a $rank_{\mathrm{R}}$ based on its performance rank and the rank of its corresponding reference point R_{cos}. In the following steps, P_t is separated to $P_t = P_t^{in} \cup P_t^{out}$. If $P_t^{in} \neq \emptyset$, the 2nd ranking criterion and adaptive selection works to lead a uniform distribution on the PF within the region. In the following sections, the key procedures of HMOEA-T are to be described in detail.

Algorithm 1 Framework of the Proposed HMOEA-T

Input: maximal number of generations t_{max}, population size N, target region T, number of objectives M.
Output: final population P_{tmax}

1: /* Initialization */
2: $\bigwedge \leftarrow$ GenerateReferencePoints()
3: $\bigwedge \leftarrow$ RegulateReferencePoints()
4: $P_0 \leftarrow$ InitializePopulation()
5: /* Main Loop */
6: $t \leftarrow 0$
7: **While** $t < t_{max}$ **do**
8: $Q_t \leftarrow$ OffspringGeneration(P_t)
9: $P_t \leftarrow P_t \cup Q_t$
10: $S_t \leftarrow$ Pareto-Nondominated_Sort(P_t) /* 1st Criterion */
11: $rank_{\mathrm{R}}() \leftarrow$ ReferencePoints-Guided_Ranking (T, S_t)/* 3rd Criterion */
12: **for** $P_t^{in} \in T$ **do**
13: $rank_{\mathrm{S}}() \leftarrow$ Strengthened Dominance Relation-Based_Ranking(P_t^{in}) /* 2nd Criterion */
14: $P_{t+1}^{in} \leftarrow$ Adaptive-Selection(P_t^{in}, N_t^{in}) /*N_t^{in} denotes to the size of P_t^{in}*/
15: **end for**
16: $P_{t+1} \leftarrow$ Reference Points-Guided_Selection(S_t, P_{t+1}^{in})
17: t $\leftarrow$ t+1
18: **end while**

B. PREFERENCE MODEL CONSTRUCTION

Target region is an intuitive and user-friendly form to express the preference information, while the reference points can concisely reflect the preference degree to each objective. In this section, we construct a preference model to take advantages of the both preference articulation method. Firstly, a set of well-distributed reference points are generated on the unit hyperplane. Then, the reference points are regulated towards the target region predefined by the DM, and locate on the unit hypersphere. In this paper, the canonical simplex-lattice design method [40] is used to generate the original uniform reference points on the hyperplane $\sum_{i=1}^{M} f_i = 1$. Suppose H be the divisions on each axis, a set of reference points $\Lambda = \{\lambda_1, \lambda_2, \ldots, \lambda_N\}$ in M-dimensional space can be obtained by

$$\begin{cases} \lambda_{i,j} \in \{\dfrac{0}{H}, \dfrac{1}{H}, \ldots, \dfrac{H}{H}\}, \\ \lambda_i = (\lambda_{i,1}, \lambda_{i,2}, \ldots, \lambda_{i,M}), \\ \sum\limits_{j=1}^{M} \lambda_j = 1 \end{cases} \tag{6}$$

where $i = 1, 2, \ldots, N$ with N being the number of uniformly distributed points. As suggested in [21], the number

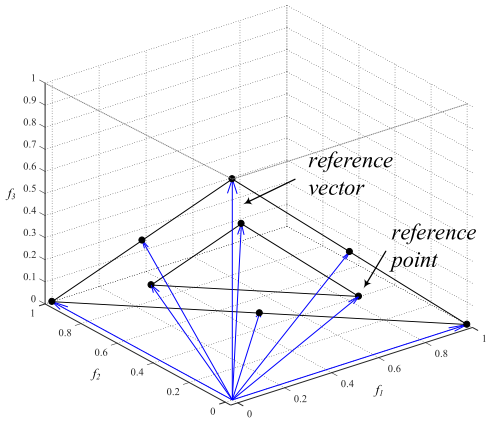

FIGURE 4. Initial distribution of reference points on the unit hyperplane in 3-D objective space.

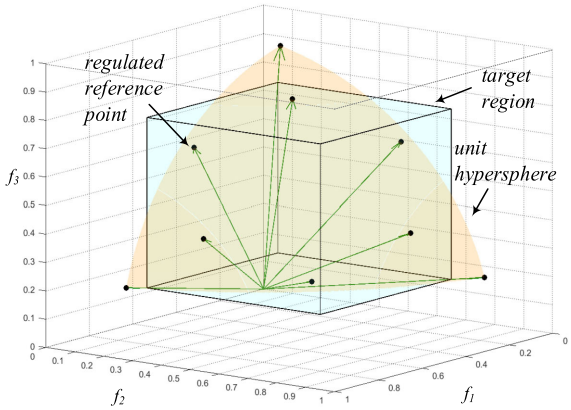

FIGURE 5. Construction of preference model in the 3-D objective space.

of two-layered reference points can be calculated as

$$N = \binom{H_1 + M - 1}{M - 1} + \binom{H_2 + M - 1}{M - 1} \tag{7}$$

where H_1 and H_2 denotes the divisions on the boundary and inner layer respectively. Fig. 4 shows the initial distribution of the reference points on the unit hyperplane with $H_1 = 2$ and $H_2 = 1$, the blue lines denotes the corresponding reference vectors.

Then, the distribution of the reference points are regulated according to the target region by (8)

$$\lambda_{i,j}^{temp} = \lambda_{i,j} \cdot LP\left(f_j\right) + x_j^L \tag{8}$$

where $LP\left(f_j\right) = x_j^U - x_j^L$ is the preference range of target region on j_{th} dimension, x_j^U and x_j^L denotes the upper and lower bound of the preference range, $\lambda_{i,j}^{temp}$ is the regulated reference point. Then, the corresponding unit reference point can be obtained by the coordinate transformation (9)

$$\lambda_{i,j}^{'} = \frac{\lambda_{i,j}^{temp}}{\left\| \lambda_{i,j}^{temp} \right\|} \tag{9}$$

Finally, under the constraint of target region, $\lambda_1^{'}, \lambda_2^{'}, \ldots, \lambda_N^{'}$ are all located at the hypersphere $\sum_{i=1}^{M} f_i^2 = 1$.

Fig. 5 shows the regulated distribution of the reference points. The blue box denotes the target region and the orange spherical represents the unit hypersphere. It can be observed that the initial reference points are transformed towards the target region and located on the unit hypersphere, hence the preference model is constructed in combination of the target region and reference points. The vector from the origin to regulated boundary reference points corresponds to the lower bound of the target region. On the other hand, when the regulation is performed under the condition that the preference range on different objectives is inconsistent, the reference points are more densely distributed on the objective with a shorter preference range. It means that the algorithm performs a fine-grained search on the more strictly required objective, which in line with the search demand of the decision maker.

C. REFERENCE POINTS GUIDED SELECTION

Reference points guided selection mainly works in three aspects: at the initial phase of the optimization, guiding the population to search towards the target region; at the middle phase, accelerating the evolution to the interior of target region; balancing the convergence and diversity of the solution set when the target regions have no intersection with true PF.

1) REFERENCE POINTS RANKING

Let the center of target regions be μ, for a reference point λ in the regulated reference point set $\Lambda^{'}$, the cosine similarity between μ and λ can be calculated by (10)

$$\cos\left(\theta_{\lambda\mu}\right) = \frac{\langle \lambda, \mu \rangle}{\|\lambda\| \cdot \|\mu\|} \tag{10}$$

Sorted by cosine similarity in descending order, the rank of the reference point set $R_{\cos} = \left\{r_1^{\cos}, r_2^{\cos}, \ldots, r_N^{\cos}\right\}$ is obtained, where r_i^{cos} denotes the rank of reference point λ_i.

Fig. 6 shows an example of ranking reference points based on the cosine similarity to the target region center. It can be seen that the greater the cosine similarity means the lower deviation degree to the region center, and attaching priority to the solutions close to these reference points can accelerate the evolution to the interior of the target region.

2) CLUSTERING OPERATION

Clustering is operated to population S_t at each generation. Let λ and μ be the unit vector corresponding to the reference vector and region center vector, respectively. The value objective of candidate solution x in M-dimensional space is $f(x) = (f_1(x), f_2(x), \ldots, f_M(x))$, $d_1(x)$ is the distance between origin and x, $d_2(x)$ and $d_3(x)$ is the perpendicular distance from x to λ and μ. They can be computed, respectively, as

$$d_1(x) = \|f(x) \cdot \lambda\| \tag{11}$$

$$d_2(x) = \|f(x)\| \cdot \sin\theta_\lambda \tag{12}$$

$$d_3(x) = \|f(x)\| \cdot \sin\theta_\mu \tag{13}$$

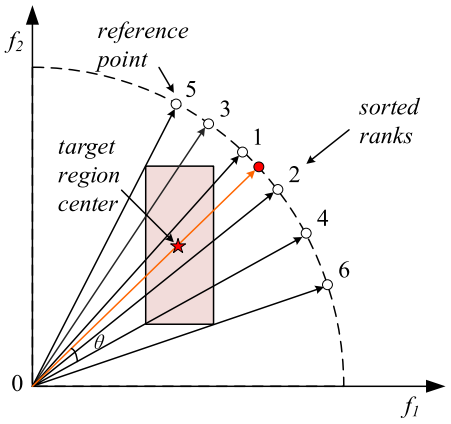

FIGURE 6. An example of ranking reference points based on the cosine similarity to target region center.

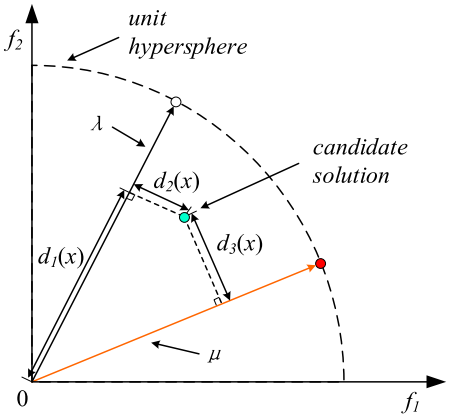

FIGURE 7. Illustration of distances $d_1(x)$, $d_2(x)$ and $d_3(x)$ in 2-D space. λ and μ denotes the reference vector and target region center vector, respectively.

where θ_λ and θ_μ is the acute angle from x to λ and μ. Fig. 7 illustrates the distance $d_1(x), d_2(x)$ and $d_3(x)$ in 2-D space. In clustering operation, only d_2 will be considered. The candidate solution x is assigned to cluster C_j with the minimum $d_{j,2}$ value. d_1 and d_3 will work in the third-level ranking assignment.

3) THIRD-LEVEL SELECTION

Once each solution in S_t is associated with a cluster among the cluster set C in clustering operation, one elitist can be selected from each cluster for the next generation. Since our motivation is to find the solution in each cluster that is closest to the ideal point while converging into the target region, the following aggregation function is proposed,

Specifically, given a translated reference point in cluster C_j, the aggregation function value of solution $x \in C_j$ can be calculated by

$$F_j(x) = d_1(x) + \varphi_1 d_2(x) + \varphi_2 d_3(x) \tag{14}$$

The smaller $d_2(x)$ means closer distance to the reference point, which eventually leads to a more uniform distribution of solution set; the smaller $d_1(x)$ under the condition

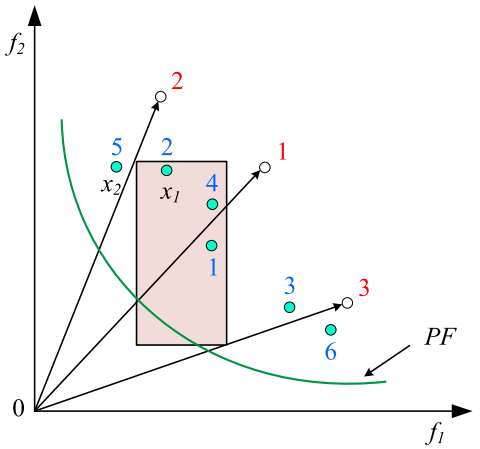

FIGURE 8. Example of third-level ranking assignment. white and blue points represents the reference points and candidate solution; the red and blue number denotes the rank of reference points and solutions, respectively.

of constant $d_1(x)$ reveals better convergence. The combination of $d_1(x)$ and $d_2(x)$ can well balance the convergence and distribution of the solution set in the objective space [42].

However, the outer layer regulated reference points correspond to the lower boundary of the target region. If only $d_1(x)$ and $d_2(x)$ are considered, the solution outside the target area but having relatively small values of $d_1(x)$ and $d_2(x)$ would be selected (such as the solution x_1 and x_2 shown in Fig. 8). Therefore, a perpendicular distance $d_3(x)$ from candidate solution x to the region center vector μ is introduced. The introduction of $d_3(x)$ makes the population tends to converge toward the region center during the search process. The smaller $F_j(x)$ value means the solution x is closer to the region center while having better convergence and distribution. And the clustering operation ensures that the closeness to region center would not be over-emphasized. Sorted in ascending order according to the $F_j(x)$ values, the rank of the solution in each cluster $R_{cls} = \left\{r_1^{cls}, r_2^{cls}, \ldots, r_{N_j}^{cls}\right\}$ is obtained, where N_j denotes the size of cluster C_j. Hence, the third-level rank of solutions in population S_t can be computed as

$$rank_R(x) = R_{\cos} + N_C \cdot (R_{cls} - 1) \tag{15}$$

In Fig. 8, the red and blue number denotes the rank of reference points and third-level rank of solution set, respectively. It can be observed that with the introduction of $d_3(x)$, x_1 is prior selected than x_2 to construct the next generation population. As suggested in [42], parameter φ_1 is set to be 5, and the influence of φ_2 will be further discussed in Section IV-D.

The set P_t^2 is used to preserve the solutions selected in second-level selection, N_t and N_t^S represents the size of P_t^2 and S_t. The rest N_t^S-N_t solutions in S_t are selected according to the third-level rank.

Then the population for next generation $P_{t+1} = P_t^2 \cup P_t^3$ is generated, where P_t^3 denotes solutions selected in third-level selection. If $P_t^{in} = \emptyset$, the reference points guided

selection works to focus the search process towards the target region; if $P_t^{in} \neq \emptyset \ \wedge \ N_t^{in} < N$, the selection mechanism attach priority to the elite solutions located within the preference region. As illustrated in Fig. 8, suppose one solution is obtained in second-level selection, the solutions ranking 1 and 2 would be prior selected, while the solution with rank 3 is de-emphasized. The combination of second-level and third-level selection can accelerate the search into the target region in the middle phase of optimization.

D. STRENGTHENED PARETO RELATION-BASED SELECTION

In application, the predefined target region usually only has a limited interaction with the true Pareto optimal front. The recently proposed strengthened Pareto relation [43] (SDR) can adapt to various shapes of Pareto fronts without any aggregation function or weight vector. We use the adaptive feature of SDR to focus search to the preferred fraction of PF instead of the entire region.

For the solutions within the target region P_t^{in}, a candidate solution x is said to dominate another candidate solution y (denoted as $x \prec_{SDR} y$) if and only if,

$$\begin{cases} Con(x) < Con(y) & \theta_{xy} \leq \overline{\theta} \\ Con(x) \cdot \frac{\theta_{xy}}{\overline{\theta}} < Con(y) & \theta_{xy} > \overline{\theta} \end{cases} \tag{16}$$

where $Con(x) = \sum_{i=1}^{M} f_i(x)$ is a metric to measure convergence degree of x, θ_{xy} denotes the acute angle between the objective values of the two candidate solutions and can be calculated by

$$\theta_{xy} = \arccos(f(x), f(y)) \tag{17}$$

and $\overline{\theta}$ is the adaptive niche size estimated according to the distribution of candidate solution set. In each niche, only one solution with best performance will be selected. To guarantee the environmental selection pressure, we choose half solutions of the P_t^{in} with well convergence and distribution performance as P_{t+1}^{in}. Hence, the size of $\overline{\theta}$ is set to be the $\lfloor N/2 \rfloor$-*th* minimum element of

$$\left\{ \min_{n \in P_t^{in} \wedge n \notin \{m\}} \theta_{mn} \ \middle| \ m \in P_t^{in} \right\} \tag{18}$$

where θ_{mn} denotes the acute angle between any pair of candidate solutions m and n, then the ratio of the non-dominated solutions in P_t^{in} is around 0.5.

Crowding distance is used in [43] to enhance diversity of the PS, which has been demonstrated ineffective in handing MaOPs [44]. SDR works in the normalized space, hence we adapt the diversity enhancement strategy in NSGA-III [21] to replace the crowding distance.

E. INTERACTIVE APPROACH BASED ON FUZZY THEORY

In practical application, the predefined preference ranges on each objectives may be too strict or loose due to the reason that the DM does not know the possibilities and limitations of the problem beforehand. Moreover, if the target region is improperly defined, the population could not reach into the preferred region, but the final solutions can still reveal the information of the closest part of true PF. Therefore, an interactive approach based on fuzzy theory is proposed in this section, whose framework is shown in Fig. 9.

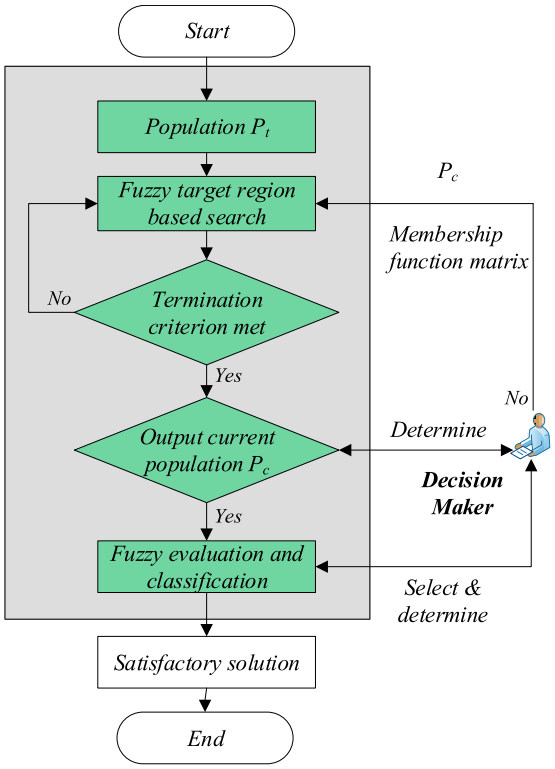

FIGURE 9. Framework of interactive approach based on fuzzy theory.

First, the preference degree on different part of the objective space is expressed. Then, the distribution of the reference points is further adapted based on the preference degree, assigning more computational resource on the sub- region with higher preference degree. Finally, the final population is classified based on the fuzzy membership matrix, helping the DM to select the most satisfied solution. The detailed steps are described as follows:

1) Input the solution sets and desirability grade

Let the M-dimensional approximate solution set obtained in previous optimization be $P_t = (x_1, x_2, \ldots, x_M)$, and each element of P_t contains N solution $x_i = (x_{i,1}, x_{i,2}, \ldots, x_{i,M})$, $i = 1, 2, \ldots, N$; $T = \{t_1, t_2, \ldots, t_P\}$ refers to the P factors describing each approximate solution; the Q desirability grade from high to low are denoted by $V = \{v_1, v_2, \ldots, v_Q\}$.

2) Membership function matrix construction

Let the fuzzy triangle membership function of factor t_p to desirability grade v_q be $a_{p,q} = (l_{p,q}, m_{p,q}, u_{p,q})$, where $l_{p,q}$ and u_{pq} is the lower and upper bound of the fuzzy triangle membership function, respectively. Larger $u_{p,q} - l_{p,q}$ refers to the higher fuzzy degree. Then, the fuzzy membership matrix

of M objective A_i can be expressed as follows,

$$A_i = (a_{p,q})_{PQ} = \begin{bmatrix} a_{1,1} & a_{1,2} & \cdots & a_{1,Q} \\ a_{2,1} & a_{2,2} & \cdots & a_{2,Q} \\ \vdots & \vdots & \ddots & \vdots \\ a_{P,1} & a_{P,2} & \cdots & a_{P,Q} \end{bmatrix} \quad (19)$$

where $p = 1, 2, \ldots, P$; $q = 1, 2, \ldots, Q$.

3) Fuzzy preference region based search

To guide the more individuals search towards the sub-objective space with higher preference degree, the distribution of reference points in each sub-spaces is further adapted. The number of reference points assigned to each region is $N \cdot (1/2, 1/4, \ldots 1/2^{P-2}, 1/2^{P-1}, 1/2^{P-1})$, the boundary of preference regions corresponds to the upper and lower bound of the membership function. The sub-preference region with higher preference degree is assigned more reference points, which means more computational resources are allocated. The number of the solutions selected in each region is the same to the size of assigned reference points.

4) Fuzzy evaluation and classification

After the termination criterion is satisfied, the DM determines whether the current population P_C should be output. If not satisfied, input the adapted fuzzy preference region and current population for further search; if satisfied, output the current population as the final population. Then fuzzy membership function matrix is utilized to classify the final solutions and help the DM to selected the most satisfied solution. Based on the value of the candidate solutions in each objective, the evaluation value to the membership function matrix is determined. The membership of solution x_i to desirability grade v_q can be calculated as

$$c_{i,q} = \frac{\sum_{p=1}^{P} a_{p,q}}{P} \quad (20)$$

Finally the fuzzy membership vector of solution x_i to desirability grade set Q is obtained, and denoted by $C_{i,q} = \{c_{i,1}, c_{i,2}, \ldots, c_{i,Q}\}$. The maximum membership method is utilized in this paper to determine the rating grade. Loop this step until all the solutions in the approximate solution set P_t are classified.

IV. EXPERIMENTAL DESIGN

This section is devoted to the experimental design for investigating the performance of the proposed algorithm. Firstly, the research questions, test problems and metrics used in our experiments are given. Then we briefly introduce the algorithms employed for comparison. Finally, the visual and numerical results are presented.

A. RESEARCH QUESTIONS AND TASK

The research questions are directly related to the assessment of the improvements aimed at in the design phase of the algorithm. The main tasks of the experimental design are as follows:

- Can the search process be effectively focused on the target region predefined by the DM?
- Is the interactive approach capable of guiding the search towards preference regions with different preference degree?
- Are the results of HMOEA-T competitive to the two recently proposed preference region-based algorithms with respect to the convergence, diversity and population proportion within the region?
- How does value of the introduced parameter in aggregation function influence the search process?

TABLE 1. Main properties of selected test functions.

Problem	Quantity
DTLZ1	Linear, Multi-modal
DTLZ2	Concave
DTLZ3	Concave, Multi-modal
DTLZ4	Concave, Biased
DTLZ7	Mixed, Disconnected, Multi-modal,Scaled
ZDT3	Convex, Noncontiguous
ZDT4	Convex, Multi-modal
MaF1	Liner
MaF3	Convex, Multi-modal

B. EXPERIMENTAL SETTINGS

As the basis for the comparative study, three benchmark test suits, DTLZ [40], ZDT [45] and MaF [46] are involved in the test. These test problems have a variety of characteristics, such as having linear, mixed (convex/concave), multi-modal, dis-connected PFs, which test different abilities of an algorithm. Main properties of the selected test functions are shown in Table 1.

To quantitatively examine and compare the performance of algorithms, we adapt the inverted generational distance (IGD) metric and the hypervolume (HV) metric. IGD calculates the minimum Euclidean distance between the solution set and the uniformly distributed points on the PF, and the smaller IGD value means better performance. HV measures both diversity and convergence of a solution set in a sense, which is strictly Pareto-compliant [47]. The HV value calculates the volume of the region dominated by the solution set and bounded by the reference point. Given a reference point, larger HV value means better quality.

The calculation of IGD and HV value requires a set of uniformly distributed reference points on the entire PF. However, the preference region-based algorithms are only interested in a fraction of the PF. Hence, in the following experiments, we locate the targeted reference points on the PF as suggested in [21], then only the reference points located within the target region are preserved for further evaluation. The modified metrics are denoted by IGD-T and HV-T. In addition, ratio of the final population in the target region (PR-T) is used to show whether the population is effectively guided within the target region.

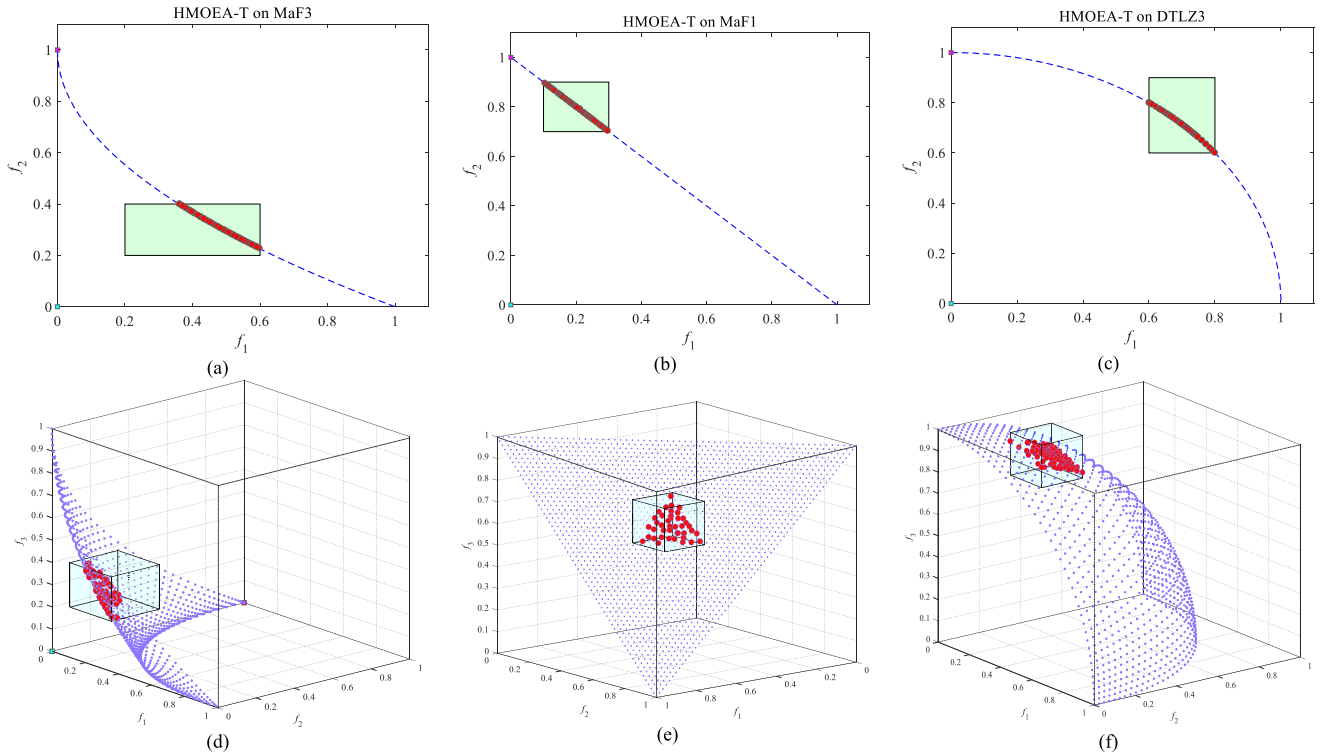

FIGURE 10. The distribution of solutions on different types of PF. The different target regions are highlighted in green box, the blue dash line denotes the true PF, the red and blue points on y axis denotes the proportion of population located within and outside the target region, respectively. (a) 2-D MaF3, convex Pareto front, (b) 2-D MaF1, linear Pareto front, (c) 2-D DTLZ3, concave Pareto front,(d) 3-D MaF3,{[0.05,0.05,0.2],[0.3,0.3,0.4]} (e) 3-D MaF1, {[0.6,0.6,0.6],[0.8,0.8,0.8]} (f) 3-D DTLZ3, {[0.2,0.2,0.8],[0.4,0.4,1]}.

The general experimental settings are listed as follows:

- The maximum number of generation (Max Gen) is used as the termination criterion. The specific number of evaluations varies due to the different computational complexity of test problems.
- The simulated binary crossover (SBX) operator and polynomial mutation (PM) operator are adopted with default parameter setting of the MOEA framework: SBX rate is 1.0, SBX distribution index is 15.0, PM rate is 1/V, where V is the number of decision variables, PM distribution index is 20.0.
- The initial population is randomly generated, and the population size are set to be 91, 210, 156, 275 for 3-, 5-, 8-, 10-objective problems.
- To distinguish the statistical difference among the results, the Wilcoxon signed-rank test [48] is performed at a 5% significance level. Each algorithm is run 20 times independently for each test.
- All the experiments are performed on the evolutionary multi-objective optimization platform PlatEMO [49], and run on the Intel 2.50 GHz Core processor with 8.0 GB of RAM.

C. ALGORITHMS IN COMPARISON

To verify the proposed HMOEA-T, two target region-based algorithms and a powerful but non-preference-based algorithm are selected.

1) T-NSGA-III [33]

T-NSGA-III integrates preference into NSGA-III in the normalization phase, where the lower bound and range of the target region are employed as the ideal point and intercepts, respectively. The solutions outside the target region would not be selected until all the solutions within the region are selected in the order of niche-preservation approach.

2) T-MOEA/D [33]

Similar to T-NSGA-III, T-MOEA/D accelerates the search process to the target region using the lower bound of target region as the ideal point. For the solutions within the target region, their fitness value are calculated and updated after the coordinate transformation. Then the fitness of solutions outside the region are added a penalty value, aiming to attach priority to solution within the region. In this paper, we employee the PBI approach among the two most commonly used methods (TCH and PBI), and the penalty value of PBI function is set to 5.

3) θ-DEA [42]

It is a reference point-based evolutionary algorithm for many-objective optimization, which can be regarded as a parameterized extension of NSGA-III. The balance between diversity and convergence are maintained by selecting only one solution with best comprehensive performance in each cluster. In this paper, θ is set to 5 as suggested in [42].

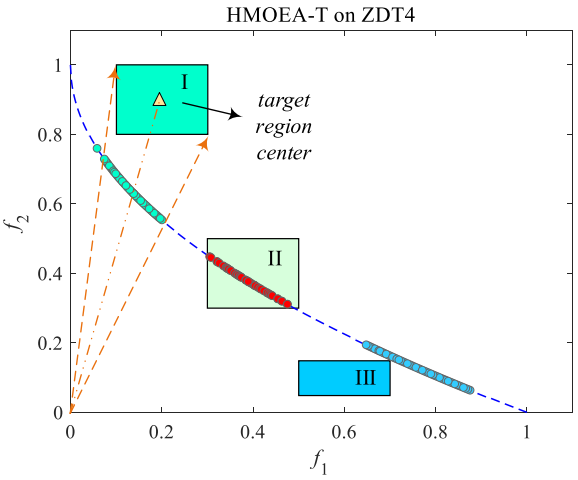

FIGURE 11. The distribution of solutions when the target regions have no intersection with the true PF. Target region I ∼ III is located in the feasible, PF and infeasible fields respectively: ZDT4.

D. VISUALIZATION AND EVALUATION

1) PRINCIPLE VERIFICATION (QUESTION 1):

In this section, the capability of HMOEA-T for focusing on the target region is visually analyzed. Fig. 10 shows the exemplary runs on MaF3, MaF1 and DTLZ3, either for a target region at the knee or the edge of the PF. The red and blue square on y axis denotes the proportion of population located within and outside the target region, respectively. It can be observed that the final solutions converge to the PF in the target region with even distribution. The tests in Fig. 10 show that the target regions can be arbitrary positioned on the convex, linear and concave PF.

In application, the DM has no idea on the location of the true Pareto front, hence the predefined target regions may have no intersection with the true PF. Under this condition, Pareto dominance and reference points work together guiding the search towards the target region. The main aim of the search is on longer obtaining evenly distributed solutions, but to find solutions closest to the target region on the PF. The experimental analysis on this case is shown in Fig. 11. Region II has interception with the PF, in which the final population successfully reached. When no PF is located in the PF, it can be observed that the final solutions cluster around the region center vector, and bordered by the upper and lower bound of the transformed reference vector. Target region I and III is located in the feasible and infeasible fields respectively, and the result indicates that the position of target region will not hinder the population from converging to the PF. It means that even the target region is improperly defined, the algorithm can still reveal the information of PF closest to the region, which is useful in the interactive phase.

Next, we select ZDT3 and DTLZ7 to test the performance of HMOEA-T on the disconnected and mixed PF. Fig. 12 shows the representative PF approximations of HMOEA-T on ZDT3 and DTLZ7. The PF of ZDT3 consists of five noncontiguous convex parts, and the PF of 2-objective

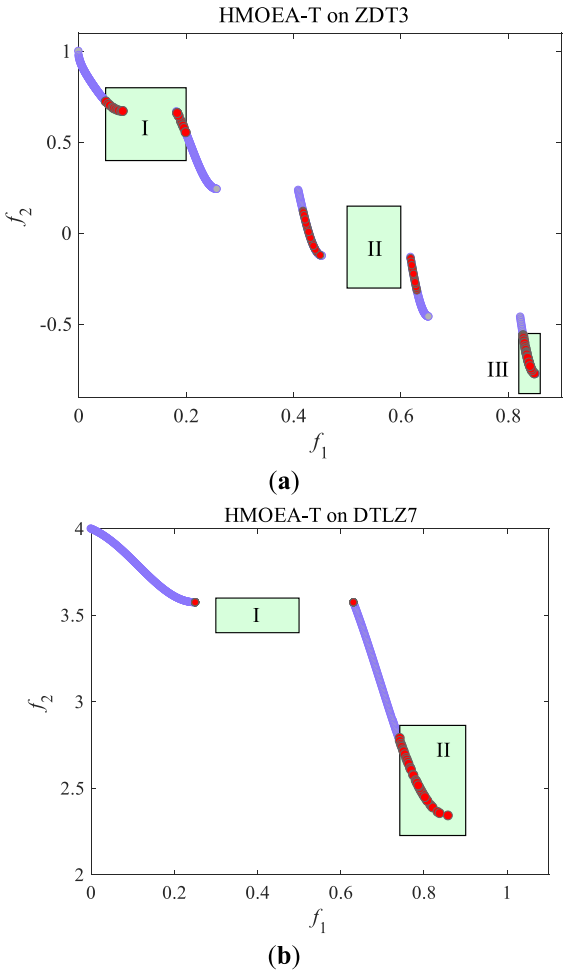

FIGURE 12. Representative PF approximations of HMOEA-T on disconnected PF. (a) 2-D ZDT3, disconnected Pareto front, (b) 2-D DTLZ7, disconnected, multi-modal Pareto front.

DTLZ7 has two disconnected and mixed part of PF. Several target regions are positioned to have two, none and one intersection part with the true PF. It can be observed that HMOEA-T successfully reach to the PF in the target region or nearest to the region, while obtaining well-distribution. The disconnection of PF in the region will not result in clustering to the local optimal solution.

Then, to validate the effectiveness of the proposed method in high-dimensional space, we select a relatively difficult 8-objective DTLZ3 problem which introduces many local optima paralleling to the global PF. Moreover, the capability of the algorithm for handling multiple target regions is also tested in this experiment.

As listed in Table 2, the DM define the preference ranges of four target regions on objective 1, 3, 6 and 8. The population size is set to be 176, and 44 reference points are assigned for each target region.

To intuitively analysis whether the population is effectively guided into each target region, the visualization method introduced in Section II-D is utilized. As shown is Fig. 13, only four cluster centers can be observed between pairwise axis,

TABLE 2. Setting of target regions in multiple regions searching, preference ranges are shown in (L, U), where 'L' and 'U' denotes lower and upper bound on each objective.

Dimension No.	I	II	III	IV
1	(0.4, 1)	(0.2, 0.9)	(0.4, 1)	(0, 0.4)
3	(0.2, 0.6)	(0, 0.4)	(0.6, 1)	(0.3, 0.9)
6	(0, 0.5)	(0.3, 0.7)	(0, 0.6)	(0.5, 1)
8	(0.3,0.9)	(0.5, 1)	(0, 0.4)	(0.2, 0.7)

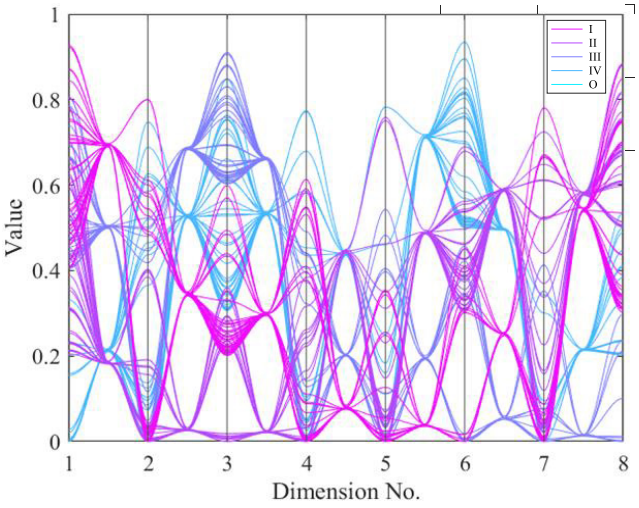

FIGURE 13. Representative results of HMOEA-T on 8-objective DTLZ3 handling four target regions. Solutions in each target are differently colored, and the solutions outside the target region would be colored cyan.

and no cyan lines appear in the plot. It means that all the individuals of the population eventually reach to their targeted preference region.

Moreover, a biased distribution can be observed on some objectives in each target region. The reason lies in two aspects: the final results depend on the preference information as well as the trade-off between the objectives. If the target region is not properly defined, a relative uniform distribution on certain objectives could sacrifice the diversity on other preference ranges; the number of approximate solutions required to describe the PF grows exponentially with the number of objectives, while only 44 solutions is used in this experiment, which may be not enough to shape the preferred PF. Summarizing the results, it can be stated that HMOEA-T is effective in high-dimensional space, and easy to extend to handle multiple target regions.

2) INTERACTIVE APPROACH (QUESTION 2):

In practical applications, the DM usually have limited information of the location and shape of the true Pareto optimal front. And the results in the former section shows that the improperly defined target regions can still reveal the information of the PF closest to the region center. The interactive approach makes it possible for the decision maker to involve in the process, learn about the potential solutions

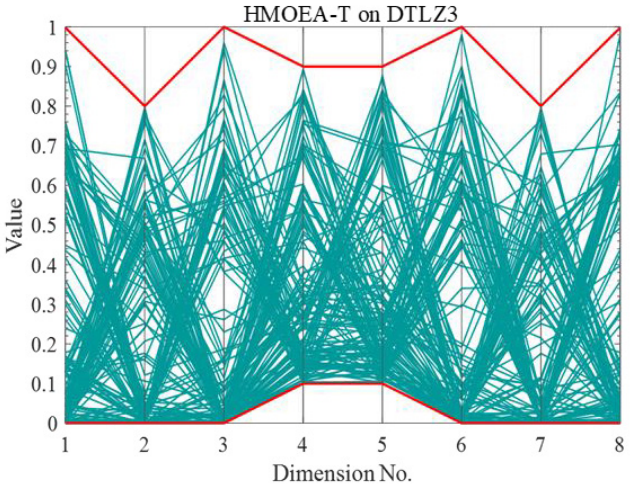

FIGURE 14. Parallel coordinate plot of the non-dominated solution set obtained by HMOEA-T on 8-objective DTLZ3. The red polylines denotes to the bounds of preference region.

TABLE 3. The triangular membership function matrix.

Dimension No.	I	II	III	IV
1	(0.2,0.3,0.6)	(0.4,0.7,0.8)	(0,0.1,0.3)	(0.9,0.9,1)
6	(0.5,0.6,0.8)	(0,0.2,0.4)	(0.6,0.9,1)	(0.3,0.4,0.6)

and fine-tune the preference region if needed. In this section, the experiments is operated on the 8-objective DTLZ3 problem. Firstly, a rough preference range {[0, 0.1, 0.1, 0], [0.8, 0.9, 0.9, 0.8]} is defined on 2nd, 4th, 5th, 7th dimension, out of which can be regarded as an unacceptable objective space. We set population size to be 288, and after 20000 function evaluations, all the solutions converge into the rough preference region as visualized in Fig. 14.

After all the solutions are guided into the acceptable objective space, the preference degree of DM on the 1st and 6th dimension is further specified in the form of triangular membership function matrix as listed in Table 3. Then the original preference region is divided into I-IV four sub-preference regions, and 144, 72, 36, 36 regulated reference points are assigned to the regions according to the region preference degree from high to low.

The distribution of solutions in target region I to IV are sequentially shown from (a) ∼ (d) in Fig. 15, where the red lines and blue lines represents the solutions inside and outside the preference region. We can observe that all the solutions in preference region I, II converge into the preference region. However, 3/36 and 35/36 of the solutions are located outside the preference region III and IV. In preference region IV, the proportion of over 97% of the outside solutions means the region has little intersection with the true PF. Hence the DM observe the distribution of the solutions and adapt the preference information for more reasonable results. It can be observed that on the 6th objective, all the solutions converge

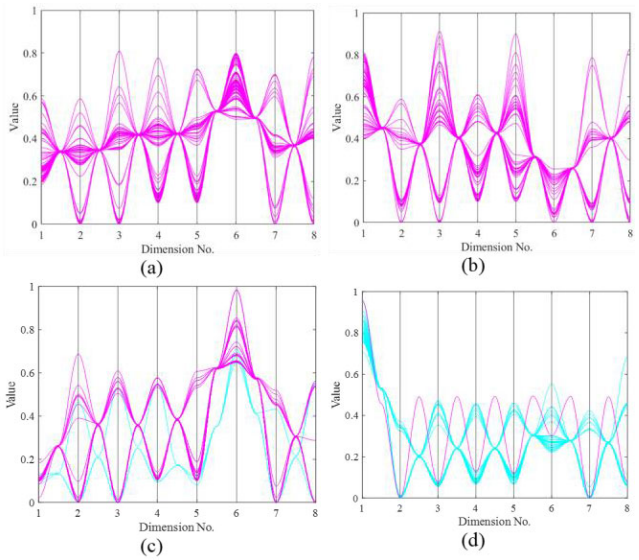

FIGURE 15. The distribution of solutions in different preference regions after first interact. The solutions located within and outside the preference region are represented in red and blue curves, respectively. (a) Preference region I; (b) Preference region II; (c) Preference region III; (d) Preference region IV.

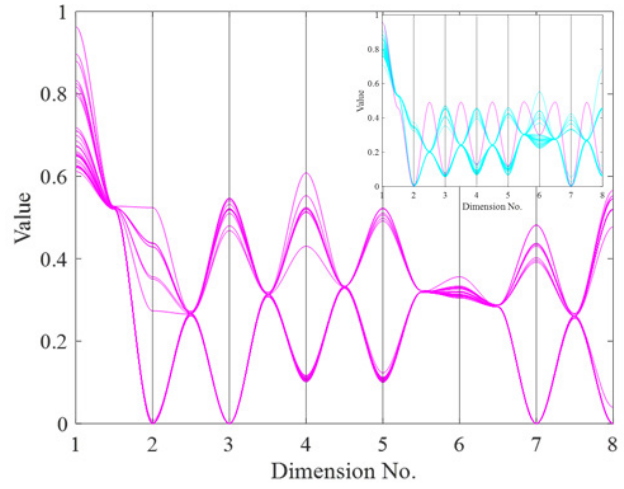

FIGURE 16. The distribution of solutions in preference region IV after interaction, and the original distribution is shown in upper right corner of the plot.

into the preference range [0.3, 0.6], while the objective value varies from 0.6 to 1 on the 1st dimension. Therefore, the DM loose the lower bound on 1st dimension to 0.6.

With another 500 generation evaluations, all the solutions reach to the preference region IV, as shown in Fig. 16.

As illustrated in Fig. 17, it can be seen that from preference region IV to region I, the size of each sub- population is increasing, indicating that the population has a higher search and aggregation degree in regions with higher preference, and its distribution is more uniform. The reason lies in that the regions with higher preferences are allocated more computing resources and individuals to approximate the true PF which located within the region. The lines O are the three individuals

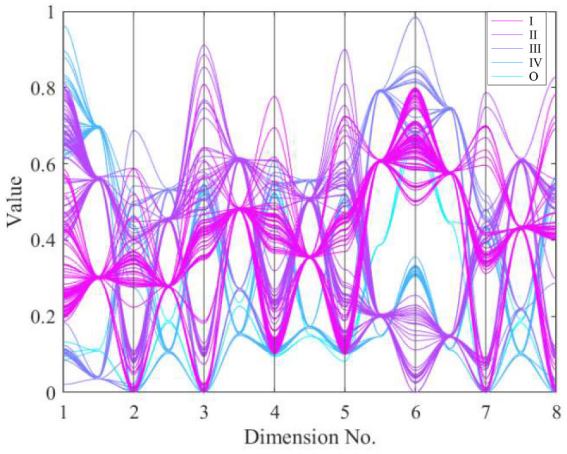

FIGURE 17. The distribution of solutions in preference region IV after interaction, and the original distribution is shown in upper right corner of the plot.

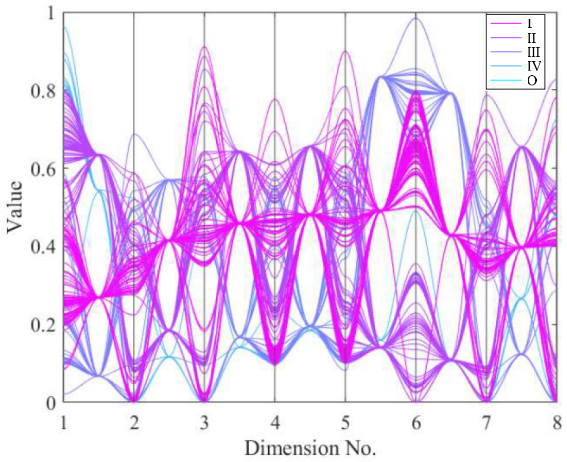

FIGURE 18. Final solution classification based on fuzzy theory.

located outside the preference region III in Fig. 15 (c), which we reserve for further analysis of how the fuzzy theory help the DM in decision making phase.

After the population is guided into different fuzzy preference regions, the final solutions are classified based on the fuzzy membership function shown in Table 3. The classified final solutions are represented in Fig. 18. It can be observed that the distribution of solutions in Fig. 18 is different from Fig. 17, where the solutions are classified based on the desirability degree while the latter utilizes the objective value. Take the three solutions outside the preference region III for example, they are identified out of the preference region for the bad performance on the 6th dimension, but they are still close to the preference region. In fuzzy classification, the three solutions are classified into cluster IV due to the good performance on other objectives. Combine with the electromagnetic field visual clustering, the distribution of final solution set is intuitively presented to the DM according to the preference degree.

TABLE 4. Performance comparison between HMOAE-T, T-NSGA-III, T-MOEA/D and θ -DEA in terms of HV-T, IGD-T and PR-T mean values. Target regions are shown in {[l], [u]}, where 'l' and 'u' denotes lower and upper bound of each objective. The best and second best result in each row is shown in bold and underline respectively.

Problem	M	Target Region	Metric	HMOEA-T	T-NSGA-III	T-MOEA/D-PBI	Θ-DEA
DTLZ1	3	{[0.1 0.1 0.1],[0.2 0.2 0.2]}	HV-T	4.1500e-2 (5.42e-4)	**4.2272e-2 (7.17e-4)** +	4.1245e-2 (5.62e-4) -	3.1144e-3 (9.54e-3) -
			IGD-T	**5.2173e-3 (2.51e-4)**	5.9309e-3 (1.42e-4) -	7.3989e-3 (1.06e-4) -	1.4670e-3 (6.56e-3) +
			PR-T	1.0000e+0 (0.00e+0)	1.0000e+0 (0.00e+0) =	9.9888e-1 (3.44e-3) =	5.1532e-3 (1.37e-2) -
	5	{[0.02 0.01 0.03 0.01 0.02], [0.18 0.19 0.17 0.19 0.18]}	HV-T	**1.4205e-1 (1.99e-3)**	1.1600e-1 (8.30e-3) -	1.0108e-1 (3.66e-3) -	6.0923e-1 (7.06e-3) -
			IGD-T	**3.1542e-2 (4.41e-4)**	3.4718e-2 (1.08e-3) -	3.4526e-2 (3.11e-4) -	7.5148e-2 (2.10e-3) -
			PR-T	9.9880e-1 (2.64e-3)	1.0000e+0 (0.00e+0) +	1.0000e+0 (0.00e+0) +	3.1429e-1 (1.14e-16) -
	8	{[0.02 0.03 0.01 0.03 0.03 0.01 0.03 0.02], [0.11 0.13 0.12 0.1 0.1 0.12 0.13 0.11]}	HV-T	**4.0223e-3 (3.05e-4)**	5.4737e-4 (3.65e-4) -	8.2187e-4 (9.41e-5) -	0.0000e+0 (0.00e+0) -
			IGD-T	**3.2664e-2 (3.74e-3)**	4.2364e-2 (1.84e-2) -	4.3342e-2 (1.15e-3) -	0.0000e+0 (0.00e+0) -
			PR-T	9.9712e-1 (6.40e-3)	7.5128e-1 (4.11e-1) -	9.9968e-1 (1.43e-3) =	0.0000e+0 (0.00e+0) -
	10	{[0.03 0.05 0 0.01 0 0 0.02 0 0.04 0.1], [0.2 0.3 0.24 0.2 0.18 0.2 0.25 0.1 0.3 0.3]}	HV-T	1.4395e-01 (4.29e-3)	1.3920e-1(6.43e-2) -	**1.6629e-1(6.25e-3)** +	0.0000e+0 (0.00e+0) -
			IGD-T	**3.2700e-2 (3.58e-3)**	7.0033e-2 (3.63e-2) -	5.9274e-2 (4.29e-3) -	0.0000e+0 (0.00e+0) -
			PR-T	9.9509e-1 (3.39e-3)	9.1473e-1 (2.64e-1) -	1.0000e+0 (0.00e+0) +	0.0000e+0 (0.00e+0) -
DTLZ2	3	{[0.4 0.2 0.3],[0.8 0.6 0.7]}	HV-T	7.0266e-2 (4.28e-4)	**7.1420e-2 (3.17e-4)** +	7.1076e-2 (1.74e-4) +	3.4996e-2 (1.61e-5) -
			IGD-T	**2.3261e-2 (5.17e-4)**	2.3261e-2 (5.27e-4) +	2.7710e-2 (1.89e-4) -	6.7328e-2 (4.36e-5) -
			PR-T	1.0000e+0 (0.00e+0)	1.0000e+0 (0.00e+0) =	9.9778e-1 (4.56e-3) =	4.3956e-2 (2.14e-17) -
	5	{[0.3 0.24 0.18 0.38 0.42], [0.7 0.6 0.83 0.57 0.63]}	HV-T	1.9507e-2 (2.86e-4)	**2.0276e-2 (8.68e-5)** +	2.0227e-2 (3.76e-5) +	0.0000e+0 (0.00e+0) -
			IGD-T	6.5028e-2 (2.31e-3)	**6.3918e-2 (2.17e-3)** +	6.8144e-2 (1.76e-3) -	0.0000e+0 (0.00e+0) -
			PR-T	1.0000e+0 (0.00e+0)	1.0000e+0 (0.00e+0) =	1.0000e+0 (0.00e+0) =	0.0000e+0 (0.00e+0) -
	8	{[0.4 0.1 0.3 0.28 0 0.2 0 0.4], [0.9 0.5 0.7 0.75 1 0.6 1 0.7]}	HV-T	2.0606e-2 (4.70e-4)	2.1122e-2 (1.64e-4) +	**2.2249e-2 (3.00e-4)** +	0.0000e+0 (0.00e+0) -
			IGD-T	1.3728e-1 (2.40e-3)	1.4614e-1 (1.62e-3) -	**1.3104e-1 (5.13e-3)** +	0.0000e+0 (0.00e+0) -
			PR-T	1.0000e+0 (0.00e+0)	1.0000e+0 (0.00e+0) =	9.9968e-1 (1.43e-3) =	0.0000e+0 (0.00e+0) -
	10	{[0.1 0.2 0 0 0.2 0 0.05 0.4 0.04 0.2], [0.7 0.8 0.95 0.9 1 0.76 0.75 0.9 0.8 0.85]}	HV-T	**4.2600e-4 (8.12e-5)**	6.5375e-5 (3.32e-5) +	5.2207e-5 (3.09e-5) -	0.0000e+0 (0.00e+0) -
			IGD-T	**2.1708e-1 (9.95e-3)**	2.6190e-1 (7.73e-3) -	2.6868e-1 (3.62e-3) -	0.0000e+0 (0.00e+0) -
			PR-T	1.0000e+0 (0.00e+0)	1.0000e+0 (0.00e+0) =	1.0000e+0 (0.00e+0) =	0.0000e+0 (0.00e+0) -
DTLZ3	3	{[0.2 0.2 0.8],[0.4 0.4 1]}	HV-T	**4.0655e-2 (1.30e-3)**	3.9560e-2 (1.93e-3) -	3.9232e-2 (3.43e-3) -	2.3786e-2 (2.04e-3) -
			IGD-T	**1.5083e-2 (2.36e-3)**	1.6881e-2 (4.71e-3) -	1.8283e-2 (9.08e-3) -	5.5261e-2 (2.77e-3) -
			PR-T	1.0000e+0 (0.00e+0)	1.0000e+0 (0.00e+0) =	9.9777e-1 (7.80e-3) =	3.3516e-2 (2.46e-3) -
	5	{[0.2 0.1 0.2 0.1 0.1], [1 0.9 0.7 0.9 0.8]}	HV-T	**2.7280e-1 (5.40e-3)**	1.3238e-1 (1.23e-1) -	2.4738e-1 (2.25e-2) -	5.3908e-2 (2.82e-2) -
			IGD-T	**1.3800e-1 (3.44e-3)**	4.8386e-1 (4.36e-1) -	1.4647e-1 (9.96e-3) -	4.3879e-1 (4.70e-1) -
			PR-T	1.0000e+0 (0.00e+0)	5.5024e-1 (5.10e-1) -	9.9952e-1 (1.47e-3) =	1.8810e-2 (1.09e-2) -
	8	{[0 0.1 0 0.5 0 0 0 0], [0.5 0.9 0.7 1 0.3 0.9 0.8 0.7]}	HV-T	**3.6306e-1 (4.54e-3)**	9.2570e-2 (1.49e-1) -	2.8203e-1 (9.31e-2) -	0.0000e+0 (0.00e+0) -
			IGD-T	**2.5194e-1 (4.03e-3)**	3.0000e-1 (4.70e-1) -	2.9170e-1 (1.04e-1) -	0.0000e+0 (0.00e+0) -
			PR-T	9.9739e-1 (3.91e-3)	2.5064e-1 (4.44e-1) -	9.0194e-1 (3.02e-1) -	0.0000e+0 (0.00e+0) -
	10	{[0.05 0 0 0.4 0 0 0 0 0 0.2], [0.95 0.9 0.6 0.9 0.8 1 0.9 1 0.8 0.8]}	HV-T	**2.7372e-1 (6.29e-3)**	1.4029e-4 (4.81e-4) -	2.3282e-1 (2.77e-2) -	0.0000e+0 (0.00e+0) -
			IGD-T	**3.1037e-1 (4.11e-3)**	2.8669e+0 (1.78e+0) -	3.3026e-1 (1.28e-2) -	0.0000e+0 (0.00e+0) -
			PR-T	9.9413e-1 (3.83e-3)	1.7273e-2 (5.91e-2) -	1.0000e+0 (0.00e+0) =	0.0000e+0 (0.00e+0) -
DTLZ4	3	{[0.1 0.4 0.6],[0.3 0.7 0.9]}	HV-T	**4.9642e-2 (2.94e-2)**	4.3844e-2 (3.30e-2) +	1.3453e-2 (2.76e-2) -	2.0972e-2 (1.24e-2) -
			IGD-T	**9.2026e-3 (5.50e-3)**	8.2810e-3 (6.24e-3) +	3.1941e-3 (6.56e-3) +	4.3489e-2 (2.58e-2) -
			PR-T	7.5000e-1 (4.44e-1)	6.5000e-1 (4.89e-1) -	1.9890e-1 (4.08e-1) -	1.6484e-2 (9.76e-3) -
	5	{[0.26 0.34 0.28 0.1 0.2], [0.7 0.68 0.78 0.58 0.8]}	HV-T	1.0273e-1 (4.80e-4)	**1.0417e-1 (2.72e-4)** +	0.0000e+0 (0.00e+0) -	1.8044e-2 (4.60e-3) -
			IGD-T	**8.8757e-2 (1.94e-3)**	8.9685e-2 (1.04e-3) -	0.0000e+0 (0.00e+0) -	3.6930e-1 (5.26e-2) -
			PR-T	1.0000e+0 (0.00e+0)	1.0000e+0 (0.00e+0) =	0.0000e+0 (0.00e+0) -	8.5714e-3 (2.49e-3) -
	8	{[0.2 0 0.28 0.18 0.05 0.32 0.25 0.3], [0.58 0.45 0.64 0.68 0.6 0.7 0.7 0.6]}	HV-T	**2.2745e-2 (4.13e-4)**	2.1101e-2 (4.98e-3) -	9.4748e-4 (4.24e-3) -	0.0000e+0 (0.00e+0) -
			IGD-T	1.6044e-1 (3.88e-3)	**1.5733e-1 (3.71e-2)** +	9.7888e-3 (4.38e-2) -	0.0000e+0 (0.00e+0) -
			PR-T	9.9094e-1 (9.25e-3)	9.5000e-1 (2.24e-1) -	5.0000e-2 (2.24e-1) -	0.0000e+0 (0.00e+0) -
	10	{[0.05 0 0 0.4 0 0 0 0 0 0.2], [0.95 0.9 0.6 0.9 0.8 1 0.9 1 0.8 0.8]}	HV-T	**1.9343e-2 (3.93e-4)**	9.2936e-3 (2.09e-3) -	0.0000e+0 (0.00e+0) -	0.0000e+0 (0.00e+0) -
			IGD-T	**1.9266e-1 (5.03e-3)**	2.4528e-1 (1.73e-2) -	0.0000e+0 (0.00e+0) -	0.0000e+0 (0.00e+0) -
			PR-T	9.9033e-1 (8.95e-3)	1.0000e+0 (0.00e+0) =	0.0000e+0 (0.00e+0) -	0.0000e+0 (0.00e+0) -
+/-/≈			HV-T		7/9/0	4/12/0	0/16/0
+/-/≈			IGD-T		4/12/0	2/14/0	1/15/0
+/-/≈			PR-T		1/7/8	2/5/9	0/16/0

3) NUMERICAL COMPARISON (QUESTION 3):

In this section, HV-T, IGD-T and PR-T are used to quantitatively evaluate the algorithms, and two recently proposed target region-based MOEAs T-NSGA-III and T-MOEA/D-PBI are selected for comparison. In addition, the metric value of a non-preference integrated algorithm Θ-DEA is used as a baseline to verify the effectiveness.

Table 4 shows the results of the four algorithms on the normalized DTLZ1-4 test problems, where the mean metric

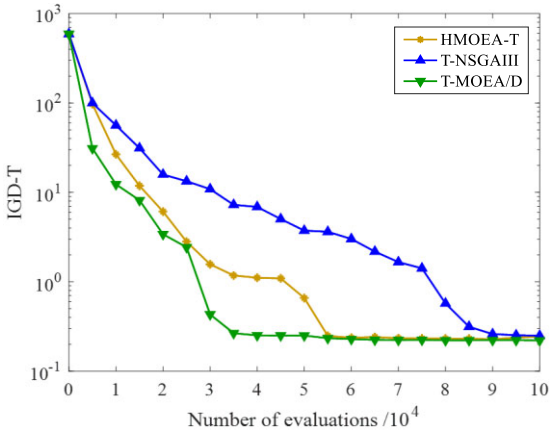

FIGURE 19. The variation of IGD-T value with number of evaluation times on 8-objective DTLZ3.

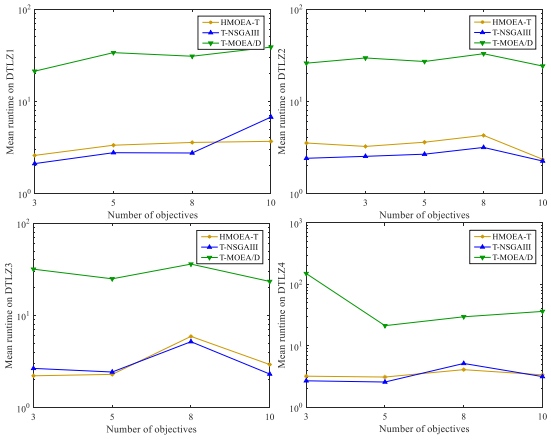

FIGURE 20. The variation of IGD-T value with number of evaluation times on 8-objective DTLZ3.

values are listed. The best and second best result in each row is shown in bold and underline respectively.

In terms of IGD-T, it can be seen that HMOEA-T performs consistently better than other algorithms on all the instances except for the 5, 8-objective DTLZ2 and 8-objective DTLZ4, but still ranks the second best on these cases. With regard to HV-T, the mean value of HMOEA-T outperforms the others on 11 out of the 16 test cases. But the algorithm shows slightly worse performance in PR-T comparison. In the cases that not all the solutions are located in the target region, the magnitude of standard deviation between the 20 runs are 10^{-3}, which means that there are always one or two outside solutions in each operation. We consider the reason is that in HMOEA-T, only half of the elite solutions are selected, while all the inside solutions are preferred than the outside solutions in the selection mechanism of T-NSGA-III and T-MOEA/D. Moreover, all the three preference-based MOEAs get better performance metric results comparing to the Θ-DEA without preference. We can observe that when the number of objectives exceeds 8, none of the solutions obtained by Θ-DEA is located in the target region.

It should be noticed that T-NSGA-III performs badly in DTLZ1 and DTLZ3, while the T-MOEA/D has trouble handling DTLZ4 problem. The proposed HMOEA-T keeps showing a stable performance among these tests. But for the 3-objective DTLZ4, none of the algorithms could achieve good performance all the time.

In addition, the variation of IGD-T value with the number of evaluation times is shown in Fig. 19. For the DTLZ3 problem which introduce a huge number of local PFs, the convergence speed of T-NSGA-III is much slower than that of HMOEA-T and T-MOEA/D.

Fig. 20 shows the variation of average run time on DTLZ1-DTLZ4. It can be observed that T-MOEA/D requires much more run time among the algorithms. The reason is that T-MOEA/D relies on the decomposition strategy, and optimization of each decomposed sub-problem is time consuming when the population size is large.

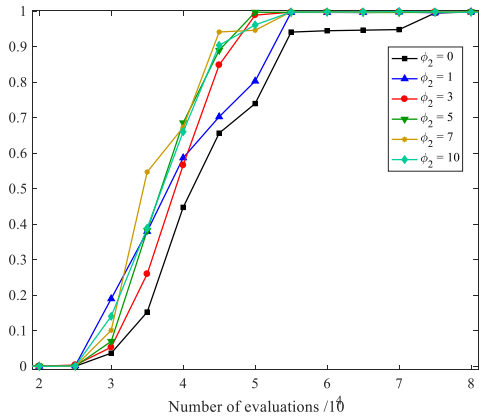

FIGURE 21. Representative examination of the influence of φ_2 on PR-T for DTLZ3 problem. The figure shows the average value of 20 independent runs.

4) INFLUENCE OF PARAMETER φ_2 (QUESTION 4):

In this section, the influence of parameter φ_2 on the performance of the algorithm is investigated. The introduction of φ_2 in reference point-guided selection aiming to accelerate the search process towards the target region, which can be revealed by the variation of PR-T value. Fig. 21 presents how the performance varies with the change of φ_2 value. We can observe that $\varphi_2 = 0$ converges slowest into the target region. At early phase of the search process, the overall convergence speed varies; when the number of evaluations reaches around 55000, all the solutions reach into the target region with the introduction of φ_2. In addition, the excessively large φ_2 may overemphasis the solution which is away from the reference point but close to the target region center, and hence lead to a worse balance between convergence and diversity. In our experiments, we set the φ_2 value to be 5.

V. CONCLUSION

In this paper, we have presented a region preference-based many-objective evolutionary algorithm called HMOEA-T, whose preference information is articulated in combination of the target region and reference point. Given a preference

region predefined by the DM, HMOEA-T is supposed to focus the search on the target region and maintain well convergence and diversity within the region. To achieve the goal, a tri-level ranking criterion is introduced into the proposed algorithm: after the Pareto dominance relation (1st rank) is considered, the solutions are guided by the regulated reference points (2nd rank) to search towards target region, then SDR-based selection adaptively maintaining convergence and diversity within the target region.

In the experimental investigation of HMOEA-T, the results show that HMOEA-T can effectively converge to the PF located in the preference region, and easy to extend to handle multiple target regions. The fuzzy theory utilized in the interactive approach enables the DM to further express the preference degree during the optimization process, and assign more computational resource on the more interested part of the objective space. Combine with the electromagnetic field visual clustering, the distribution pattern of preferred solutions is intuitively presented to help the DM analysis and find the most interested solutions. Quantitative comparison of HMOEA-T and two state-of-the-art target region-based algorithms is performed based on three metrics, which reveals that the proposed algorithm works well on most of the test cases, especially the multimodal problems. The HMOEA-T also show an superior performance with regard to the convergence speed and computation time.

In future studies, we will compare HMOEA-T with other categories of the preference-based algorithms on more benchmark problems. In some tests, the SDR-based selection struggles to obtain the diversity on the PF. So a selection mechanism is required, which can effectively distinguish the non-dominated solutions identified by SDR. Moreover, the HMOEA-T should be tested on practical applications.

REFERENCES

[1] Y. Y. Han, D. W. Gong, X. Y. Sun, and Q. K. Pan, "An improved NSGA-II algorithm for multi-objective lot-streaming flow shop scheduling problem," *Int. J. Prod. Res.*, vol. 52, no. 8, pp. 2211–2231, Apr. 2014.

[2] B. Chen, Y. Lin, W. Zeng, H. Xu, and D. Zhang, "The mean-variance cardinality constrained portfolio optimization problem using a local search-based multi-objective evolutionary algorithm," *Appl. Intell.*, vol. 47, no. 2, pp. 505–525, Sep. 2017.

[3] M. Farina and P. Amato, "On the optimal solution definition for many-criteria optimization problems," in *Proc. Annu. Meeting North Amer. Fuzzy Inf. Process. Soc. Proc.*, Jun. 2002, pp. 233–238.

[4] Y. Tian, H. Wang, X. Zhang, and Y. Jin, "Effectiveness and efficiency of non-dominated sorting for evolutionary multi- and many-objective optimization," *Complex Intell. Syst.*, vol. 3, no. 4, pp. 247–263, Dec. 2017.

[5] H. Seada and K. Deb, "Non-dominated sorting based multi/many-objective optimization: Two decades of research and application," in *Multi-Objective Optimization*, J. K. Mandal, S. Mukhopadhyay, and P. Dutta, Eds. Singapore: Springer, 2018, pp. 1–24.

[6] R. K. Pandey and S. S. Panda, "Optimization of bone drilling using Taguchi methodology coupled with fuzzy based desirability function approach," *J. Intell. Manuf.*, vol. 26, no. 6, pp. 1121–1129, Dec. 2015.

[7] C. Buratti, M. Barbanera, E. Lascaro, and F. Cotana, "Optimization of torrefaction conditions of coffee industry residues using desirability function approach," *Waste Manage.*, vol. 73, pp. 523–534, Mar. 2018.

[8] L. Jiao, W. Zhang, R. Liu, and F. Liu, "A hybrid multiobjective immune algorithm with region preference for decision makers," in *Proc. IEEE Congr. Evol. Comput.*, Jul. 2010, pp. 1–8.

[9] A. Camacho, G. Toscano, R. Landa, and H. Ishibuchi, "Indicator-based weight adaptation for solving many-objective optimization problems," in *Proc. Int. Conf. Evol. Multi-Criterion Optim.*, 2019, pp. 216–228.

[10] K. Deb and J. Sundar, "Reference point based multi-objective optimization using evolutionary algorithms," in *Proc. 8th Annu. Conf. Genetic Evol. Comput.*, Jul. 2006, pp. 635–642.

[11] E. Fernandez, E. Lopez, S. Bernal, C. A. C. Coello, J. Navarro, and O. Research, "Evolutionary multiobjective optimization using an outranking-based dominance generalization," *Comput. Oper. Res.*, vol. 37, no. 2, pp. 390–395, Feb. 2010.

[12] T. Wagner, H. Trautmann, and D. Brockhoff, "Preference articulation by means of the R2 indicator," in *Proc. Int. Conf. Evol. Multi-Criterion Optim.*, Mar. 2013, pp. 81–95.

[13] O. Schutze, X. Esquivel, A. Lara, and C. A. C. Coello, "Using the averaged Hausdorff distance as a performance measure in evolutionary multiobjective optimization," *IEEE Trans. Evol. Comput.*, vol. 16, no. 4, pp. 504–522, Aug. 2012.

[14] C. M. Fonseca and P. J. Fleming, "Genetic Algorithms for Multiobjective Optimization: FormulationDiscussion and Generalization," in *Proc. ICGA*, Jul. 1993, pp. 416–423.

[15] C. M. Fonseca and P. J. Fleming, "Multiobjective optimization and multiple constraint handling with evolutionary algorithms: I. A unified formulation," *IEEE Trans. Syst., Man, Cybern. A, Syst. Hum.*, vol. 28, no. 1, pp. 26–37, Jan. 1998.

[16] K. C. Tan, T. H. Lee, and E. F. Khor, "Evolutionary algorithms with goal and priority information for multi-objective optimization," in *Proc. Congr. Evol. Comput.*, vol. 1, Jul. 1999, pp. 106–113.

[17] J. Molina, L. V. Santana, A. G. Hernández-Díaz, C. A. C. Coello, and R. Caballero, "g-dominance: Reference point based dominance for multiobjective metaheuristics," *Eur. J. Oper. Res.*, vol. 197, no. 2, pp. 685–692, Sep. 2009.

[18] R. C. Purshouse, K. Deb, M. M. Mansor, S. Mostaghim, and R. Wang, "A review of hybrid evolutionary multiple criteria decision making methods," in *Proc. IEEE Congr. Evol. Comput. (CEC)*, Jul. 2014, pp. 1147–1154.

[19] F. Goulart and F. Campelo, "Preference-guided evolutionary algorithms for many-objective optimization," *Inf. Sci.*, vol. 329, pp. 236–255, Feb. 2016.

[20] Q. Fei-yue, W. Yu-shi, W. Li-ping, and J. Bo, "Bipolar preferences dominance based evolutionary algorithm for many-objective optimization," in *Proc. IEEE Congr. Evol. Comput.*, Jun. 2012, pp. 1–8.

[21] K. Deb and H. Jain, "An evolutionary many-objective optimization algorithm using reference-point-based nondominated sorting approach, part I: Solving problems with box constraints," *IEEE Trans. Evol. Comput.*, vol. 18, no. 4, pp. 577–601, Apr. 2013.

[22] L. Cai, S. Qu, Y. Yuan, and X. Yao, "A clustering-ranking method for many-objective optimization," *Appl. Soft Comput.*, vol. 35, pp. 681–694, Oct. 2015.

[23] Y. Zhao, J. Liu, X. Yu, F. Li, and J. Zhu, "Many-objective particle swarm optimization algorithm based on preference," in *Proc. 37th Chin. Control Conf. (CCC)*, Jul. 2018, pp. 3168–3174.

[24] R. Hernández Gómez and C. A. Coello Coello, "Improved metaheuristic based on the R2 indicator for many-objective optimization," in *Proc. Annu. Conf. Genetic Evol. Comput.*, Jul. 2015, pp. 679–686.

[25] G. Rudolph, O. Schütze, C. Grimme, and H. Trautmann, "An aspiration set EMOA based on averaged Hausdorff distances," in *Learning and Intelligent Optimization—LION* (Lecture Notes in Computer Science), vol. 8426, P. Pardalos, M. Resende, C. Vogiatzis, and J. Walteros, Eds. Cham, Switzerland: Springer, 2014.

[26] Y. Wang, L. Li, K. Yang, and M. T. Emmerich, "A new approach to target region based multiobjective evolutionary algorithms," in *Proc. IEEE Congr. Evol. Comput. (CEC)*, Jun. 2017, pp. 1757–1764.

[27] H. Trautmann and J. Mehnen, "Preference-based Pareto optimization in certain and noisy environments," *Eng. Optim.*, vol. 41, no. 1, pp. 23–38, Jan. 2009.

[28] I. Giagkiozis, R. C. Purshouse, and P. J. Fleming, "Generalized decomposition and cross entropy methods for many-objective optimization," *Inf. Sci.*, vol. 282, pp. 363–387, Oct. 2014.

[29] K. Deb and A. Kumar, "Interactive evolutionary multi-objective optimization and decision-making using reference direction method," in *Proc. 9th Annu. Conf. Genetic Evol. Comput.*, Jul. 2007, pp. 781–788.

[30] T. Wagner and H. Trautmann, "Integration of preferences in hypervolume-based multiobjective evolutionary algorithms by means of desirability functions," *IEEE Trans. Evol. Comput.*, vol. 14, no. 5, pp. 688–701, Oct. 2010.

[31] H. Trautmann, T. Wagner, D. Biermann, and C. Weihs, "Indicator-based selection in evolutionary multiobjective optimization algorithms based on the desirability index," *J. Multi-Criteria Decis. Anal.*, vol. 20, nos. 5–6, pp. 319–337, Sep. 2013.
[32] L. Li, Y. Wang, H. Trautmann, N. Jing, and M. Emmerich, "Multiobjective evolutionary algorithms based on target region preferences," *Swarm Evol. Comput.*, vol. 40, pp. 196–215, Jun. 2018.
[33] L. Li, H. Chen, J. Li, N. Jing, and M. Emmerich, "Preference-based evolutionary many-objective optimization for agile satellite mission planning," *IEEE Access*, vol. 6, pp. 40963–40978, 2018.
[34] R. Cheng, Y. Jin, M. Olhofer, and B. Sendhoff, "A reference vector guided evolutionary algorithm for many-objective optimization," *IEEE Trans. Evol. Comput.*, vol. 20, no. 5, pp. 773–791, Oct. 2016.
[35] M. Gong, F. Liu, W. Zhang, L. Jiao, and Q. Zhang, "Interactive MOEA/D for multi-objective decision making," in *Proc. 13th Annu. Conf. Genetic Evol. Comput.*, Jul. 2011, pp. 721–728.
[36] L. B. Said, S. Bechikh, and K. Ghédira, "The r-dominance: A new dominance relation for interactive evolutionary multicriteria decision making," *IEEE Trans. Evol. Comput.*, vol. 14, no. 5, pp. 801–818, Oct. 2010.
[37] A. López-Jaimes and C. A. C. Coello, "Including preferences into a multiobjective evolutionary algorithm to deal with many-objective engineering optimization problems," *Inf. Sci.*, vol. 277, pp. 1–20, Sep. 2014.
[38] F. Liu, K. Tian, Y. Sun, B. Y. Li, and H. Lin, "Analysis of statistics data based on mixed visualization techniques," *Appl. Mech. Mater.*, vols. 220–223, pp. 2479–2484, Nov. 2012.
[39] B. Morvay and L. Pálfalvi, "On the applicability of Ampère's law," *Eur. J. Phys.*, vol. 36, no. 6, Sep. 2015, Art. no. 065014.
[40] K. Deb, L. Thiele, M. Laumanns, and E. Zitzler, "Scalable multi-objective optimization test problems," in *Proc. Congr. Evol. Comput.*, May 2002, pp. 825–830.
[41] J. A. Cornell, *Experiments with Mixtures: Designs, Models, and the Analysis of Mixture Data*. Hoboken, NJ, USA: Wiley, 2011.
[42] Y. Yuan, H. Xu, B. Wang, and X. Yao, "A new dominance relation-based evolutionary algorithm for many-objective optimization," *IEEE Trans. Evol. Comput.*, vol. 20, no. 1, pp. 16–37, Feb. 2016.
[43] Y. Tian, R. Cheng, X. Zhang, Y. Su, and Y. Jin, "A strengthened dominance relation considering convergence and diversity for evolutionary many-objective optimization," *IEEE Trans. Evol. Comput.*, vol. 23, no. 2, pp. 331–345, Apr. 2019.
[44] M. Li, S. Yang, and X. Liu, "Shift-based density estimation for Pareto-based algorithms in many-objective optimization," *IEEE Trans. Evol. Comput.*, vol. 18, no. 3, pp. 348–365, Jun. 2014.
[45] E. Zitzler, K. Deb, and L. Thiele, "Comparison of multiobjective evolutionary algorithms: Empirical results," *Evol. Comput.*, vol. 8, no. 2, pp. 173–195, 2000.
[46] R. Cheng, M. Li, Y. Tian, X. Zhang, S. Yang, Y. Jin, and X. Yao, "A benchmark test suite for evolutionary many-objective optimization," *Complex Intell. Syst.*, vol. 3, no. 1, pp. 67–81, Mar. 2017.
[47] E. Zitzler, L. Thiele, M. Laumanns, C. M. Fonseca, and V. G. da Fonseca Grunert, "Performance assessment of multiobjective optimizers: An analysis and review," *IEEE Trans. Evol. Comput.*, vol. 7, no. 2, pp. 117–132, Apr. 2003.
[48] F. Wilcoxon, "Individual comparisons by ranking methods," *Biometrics Bull.*, vol. 1, no. 6, pp. 80–83, 1945.
[49] Y. Tian, R. Cheng, X. Zhang, and Y. Jin, "Platemo: A MATLAB platform for evolutionary multi-objective optimization [educational forum]," *IEEE Comput. Intell. Mag.*, vol. 12, no. 4, pp. 73–87, Nov. 2017.

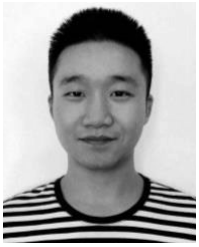

MINGHUI XIONG was born in Biyang, Henan, China, in 1995. He received the B.S. degree from the Science and Technology on Complex Electronic System Simulation Laboratory, Space Engineering University, Space Engineering University, in 2017, where he is currently pursuing the M.S. degree. His current research interests include preference modeling, evolutionary many-objective optimization, and satellite constellation design.

WEI XIONG was born in 1971. He received the Ph.D. degree from Beihang University, in 2005. He is currently a Professor with the Science and Technology on Complex Electronic System Simulation Laboratory, Space Engineering University. His research interests include the complex networks, and systems engineering and theory.

CHENGXIANG LIU was born in Jiamusi, Heilongjiang, China, in 1990. He received the M.S. degree from the Aviation University of Air Force, in 2014. He is currently pursuing the Ph.D. degree with the Science and Technology on Complex Electronic System Simulation Laboratory, Space Engineering University. His current research interests include complex networks, the invulnerability of spatial information networks, and satellite constellation design.